

# Negative impact of heavy-tailed uncertainty and error distributions on the reliability of calibration statistics for machine learning regression tasks

Pascal PERNOT <sup>1</sup>

*Institut de Chimie Physique, UMR8000 CNRS,  
Université Paris-Saclay, 91405 Orsay, France<sup>a)</sup>*

Average calibration of the prediction uncertainties of machine learning regression tasks can be tested in two ways: one is to estimate the calibration error (CE) as the difference between the mean absolute error (MAE) and the mean variance (MV) or mean squared uncertainty; the alternative is to compare the mean squared z-scores (ZMS) or scaled errors to 1. The problem is that both approaches might lead to different conclusions, as illustrated in this study for an ensemble of datasets from the recent machine learning uncertainty quantification (ML-UQ) literature. It is shown that the estimation of MV, MAE and their confidence intervals can become unreliable for heavy-tailed uncertainty and error distributions, which seems to be a common issue for ML-UQ datasets. By contrast, the ZMS statistic is less sensitive and offers the most reliable approach in this context. Unfortunately, the same problem affects also *conditional* calibration statistics, such as the popular ENCE, and very likely *post-hoc* calibration methods based on similar statistics. As not much can be done to relieve this issue, except for a change of paradigm to intervals- or distribution-based UQ metrics, robust tailedness metrics are proposed to detect the potentially problematic datasets.

**This preprint is a revised and extended version of “How to validate average calibration for machine learning regression tasks?” (<https://arxiv.org/abs/2402.10043v2>).**

---

<sup>a)</sup>Electronic mail: [pascal.pernot@cnrs.fr](mailto:pascal.pernot@cnrs.fr)

## I. INTRODUCTION

The assessment of prediction uncertainty calibration for machine learning (ML) regression tasks is based on two main types of statistics: (1) the calibration errors (RCE, UCE, ENCE...) <sup>1,2</sup> which are based on the comparison of the mean squared errors (MSE) to mean squared uncertainties or mean variance (MV); and (2) the Negative Log-Likelihood (NLL) <sup>3-5</sup> which is based on the mean of squared z-scores or scaled errors (ZMS) <sup>2</sup>. The comparison of MSE to MV has been used to test or establish *average* calibration <sup>6,7</sup>, but it mostly occurs in ML through a bin-based setup <sup>1</sup>, meaning that it measures local or *conditional* calibration.

Average calibration is known to be insufficient to guarantee the reliability of uncertainties across data space <sup>8</sup>, but it remains a necessary condition that is too often overlooked in calibration studies. Moreover, an interest of the RCE and ZMS statistics is to have predefined reference values, enabling direct statistical testing of average calibration. This is not the case for bin-based statistics such as the UCE and ENCE, for which validation is much more complex <sup>9</sup>. *De facto*, the latter are practically used only in comparative studies, without validation.

This study focuses on the comparison of RCE- and ZMS-based approaches to validate calibration, and is motivated by the observation that both approaches might lead to conflicting diagnostics when applied to ML uncertainty quantification (ML-UQ) datasets. Understanding the origin of such discrepancies is important to assess the reliability of these calibration statistics and their bin-based extensions.

The next section defines the calibration statistics and the validation approach. Sect. III introduces the ML-UQ datasets used to illustrate the validation results, with a focus on the shape of their uncertainty and error distributions. Numerical experiments, based on synthetic datasets mimicking the real datasets, are performed in Sect. IV, in order establish the impact of the tailedness of the uncertainty and error distributions on the reliability of the calibration statistics. Sect. V illustrates this reliability issue on the reference ML-UQ datasets for RCE and ZMS, and estimates its impact on conditional calibration statistics. The main conclusions are presented in Sect. VI.

## II. AVERAGE CALIBRATION STATISTICS

Let us consider a dataset composed of *paired* errors and uncertainties  $\{E_i, u_{E_i}\}_{i=1}^M$  to be tested for *average* calibration. The variance-based UQ validation statistics are built on a probabilistic model linking errors to uncertainties

$$E_i \sim u_{E_i} D(0, 1) \quad (1)$$

where  $D(\mu, \sigma)$  is an unspecified probability density function with mean  $\mu$  and standard deviation  $\sigma$ . This model states that errors are expected to be unbiased ( $\mu = 0$ ) and that uncertainty quantifies the *dispersion* of errors, according to the metrological definition<sup>10</sup>.

### A. The calibration error and related statistics

Let us assume that the errors are drawn from a distribution  $D(0, \sigma)$  with an unknown scale parameter  $\sigma$ , itself distributed according to a distribution  $G$ . The distribution of errors is then a *scale mixture distribution*  $H$ , with probability density function

$$p_H(E) = \int_0^\infty p_D(E|\sigma) p_G(\sigma) d\sigma \quad (2)$$

and the variance of the compound distribution of errors is obtained by the *law of total variance*

$$\text{Var}(E) = \langle \text{Var}_D(E|\sigma) \rangle_G + \text{Var}_G(\langle E|\sigma \rangle_D) \quad (3)$$

$$= \langle u_E^2 \rangle + \text{Var}_G(\langle E|\sigma \rangle_D) \quad (4)$$

where the first term of the RHS of Eq. 3 has been identified as the mean squared uncertainty  $\langle u_E^2 \rangle$ . This expression can be compared to the standard expression for the variance

$$\text{Var}(E) = \langle E^2 \rangle - \langle E \rangle^2 \quad (5)$$

For an unbiased error distribution, one gets  $\text{Var}_G(\langle E|\sigma \rangle_D) = 0$  and  $\langle E \rangle = 0$ , leading to

$$\langle E^2 \rangle = \langle u_E^2 \rangle \quad (6)$$

Based on this equation, the Relative Calibration Error, aimed to test average calibration, is defined as

$$\text{RCE} = \frac{\text{RMV} - \text{RMSE}}{\text{RMV}} \quad (7)$$

where  $\text{RMSE}$  is the root mean squared error  $\sqrt{\langle E^2 \rangle}$  and  $\text{RMV}$  is the root mean variance ( $\sqrt{\langle u_E^2 \rangle}$ ). The reference value to validate the RCE is 0.

The RCE is rarely used as such, but it occurs in a bin-based statistic of *conditional calibration*,<sup>2</sup> the Expected Normalized Calibration Error<sup>1</sup>

$$ENCE = \frac{1}{N} \sum_{i=1}^N |RCE_i| \quad (8)$$

where  $RCE_i$  is estimated over the data in bin  $i$ . Depending on the variable chosen to design the bins, the ENCE might be used to test *consistency* (binning on  $u_E$ ) or *adaptivity* (binning on input features)<sup>2</sup>. The ENCE has no predefined reference value (it depends on the dataset and the binning scheme)<sup>9</sup>, which complicates the statistical testing of conditional calibration.

## B. ZMS and related statistics

Another approach to calibration based on Eq. 1 uses scaled errors or z-scores

$$Z_i = \frac{E_i}{u_{E_i}} \sim D(0, 1) \quad (9)$$

with the property

$$\text{Var}(Z) = 1 \quad (10)$$

assessing average calibration for unbiased errors<sup>11,12</sup>. If one accepts that the uncertainties have been tailored to cover biased errors, the calibration equation becomes

$$ZMS = \langle Z^2 \rangle = 1 \quad (11)$$

which is the preferred form for testing<sup>2</sup>, notably when a dataset is split into subsets for the assessment of conditional calibration. The target value for statistical validation of the ZMS is 1.

The negative log-likelihood (NLL) score for a normal likelihood is linked to the ZMS by<sup>13</sup>

$$NLL = \frac{1}{2} \left( \langle Z^2 \rangle + \langle \ln u_E^2 \rangle + \ln 2\pi \right) \quad (12)$$

It combines the ZMS as an *average calibration* term<sup>14</sup> to a *sharpness* term driving the uncertainties towards small values<sup>15</sup> when the NLL is used as a loss function, hence preventing the minimization of  $\langle Z^2 \rangle$  by arbitrary large uncertainties. For a given set of uncertainties, testing the NLL value is equivalent to testing the ZMS value.

As for the RCE, the ZMS can be used to validate conditional calibration through a bin-based approach, the Local ZMS (LZMS) analysis<sup>2</sup>.

### C. Validation

Considering that errors and uncertainties have generally non-normal distributions, and that it is not reliable to invoke the Central Limit Theorem to use normality-based testing approaches (see Pernot<sup>11</sup>), one has to infer confidence intervals on the statistics by bootstrapping (BS) for comparison to their reference values.

For a given dataset  $(E, u_E)$  and a statistic  $\vartheta$ , one estimates the statistic over the dataset,  $\vartheta_{est}$ , and a bootstrapped sample from which one gets the bias of the bootstrapped distribution  $b_{BS}$  and a 95% confidence interval  $I_{BS} = [I_{BS}^-, I_{BS}^+]$ . Note that it is generally not recommended to correct  $\vartheta_{est}$  from the bootstrapping bias  $b_{BS}$ , but it is important to check that the bias is negligible. One of the most reliable BS approaches in these conditions is considered to be the Bias Corrected Accelerated (BC<sub>a</sub>) method<sup>16</sup>, which is used throughout this study.

Validation is then done by checking that the target value for the statistic,  $\vartheta_{ref}$ , lies within  $I_{BS}$ , i.e.

$$\vartheta_{ref} \in [I_{BS}^-, I_{BS}^+] \quad (13)$$

To go beyond this binary result, it is interesting to have a continuous measure of agreement, and one can define a standardized score  $\zeta$  as the ratio of the signed distance of the estimated value  $\vartheta_{est}$  to its reference  $\vartheta_{ref}$ , over the absolute value of the distance between  $\vartheta_{est}$  and the limit of the confidence interval closest to  $\vartheta_{ref}$ . More concretely

$$\zeta(\vartheta_{est}, \vartheta_{ref}, I_{BS}) = \begin{cases} \frac{\vartheta_{est} - \vartheta_{ref}}{I_{BS}^+ - \vartheta_{est}} & \text{if } (\vartheta_{est} - \vartheta_{ref}) \leq 0 \\ \frac{\vartheta_{est} - \vartheta_{ref}}{\vartheta_{est} - I_{BS}^-} & \text{if } (\vartheta_{est} - \vartheta_{ref}) > 0 \end{cases} \quad (14)$$

which considers explicitly the possible asymmetry of  $I_{BS}$  around  $\vartheta_{est}$ . The compatibility of the statistic with its reference value can then be tested by

$$|\zeta(\vartheta_{est}, \vartheta_{ref}, I_{BS})| \leq 1 \quad (15)$$

which is strictly equivalent to the interval test (Eq. 13). In addition to testing,  $\zeta$ -scores provide valuable information about the sign and amplitude of the mismatch between the statistic and its reference value.

### III. ML-UQ DATASETS

Nine test sets, including errors and *calibrated* uncertainties, have been collected from the recent ML-UQ literature for the prediction of various physico-chemical properties by a di-

Set #	Name	Size $M$	Shape parameter $\nu$		
			$u_E^2$	$E^2$	$Z^2$
1	Diffusion_RF <sup>18</sup>	2040	1.72	2.17	7.91
2	Perovskite_RF <sup>18</sup>	3834	0.79	1.18	4.91
3	Diffusion_LR <sup>18</sup>	2040	5.34	6.32	15.10
4	Perovskite_LR <sup>18</sup>	3836	1.53	2.72	8.15
5	Diffusion_GPR_Bayesian <sup>18</sup>	2040	30.8	2.75	2.72
6	Perovskite_GPR_Bayesian <sup>18</sup>	3818	1.19	0.78	0.85
7	QM9_E <sup>19</sup>	13885	1.91	2.43	3.95
8	logP_10k_a_LS-GCN <sup>5</sup>	5000	24.7	4.24	3.66
9	logP_150k_LS-GCN <sup>5</sup>	5000	17.3	10.0	20.2

Table I. The nine datasets used in this study: number, name with reference, size, and shape parameters for the fits of  $u_E^2$  by an Inverse Gamma distribution, and of the  $E^2$  and  $Z^2$  by an  $F$  distribution.

verse panel of ML methods. This selection ignored small datasets and those presenting identical properties. Note that for all these datasets, the uncertainties have been calibrated by a palette of methods with various levels of success<sup>2,17</sup>. The datasets names, sizes, bibliographic references and shape statistics are gathered in Table I, and the reader is referred to the original articles for further details. In the following, a short notation is used, e.g. ‘Set 7’ corresponds to the QM9\_E dataset.

As the shape of the distributions of  $u_E^2$ ,  $E^2$  and  $Z^2$  is central to the elucidation of the problem presented in the following sections, these were characterized for each dataset as explained below and reported in Table I.

### A. $u_E^2$ distributions

The Inverse-Gamma (IG) distribution<sup>20</sup> is commonly used to describe variance ( $u_E^2$ ) samples

$$u_E^2 \sim \Gamma^{-1}(\alpha = \nu, \beta = \sigma\nu) \quad (16)$$

where  $\alpha > 0$  and  $\beta > 0$  are the shape and scale parameters, respectively, expressed as combinations of a number of degrees of freedom  $\nu$  and a scale factor  $\sigma$ . This equation is more conveniently expressed as

$$u_E^2/\sigma^2 \sim \Gamma^{-1}(\nu, \nu) \quad (17)$$

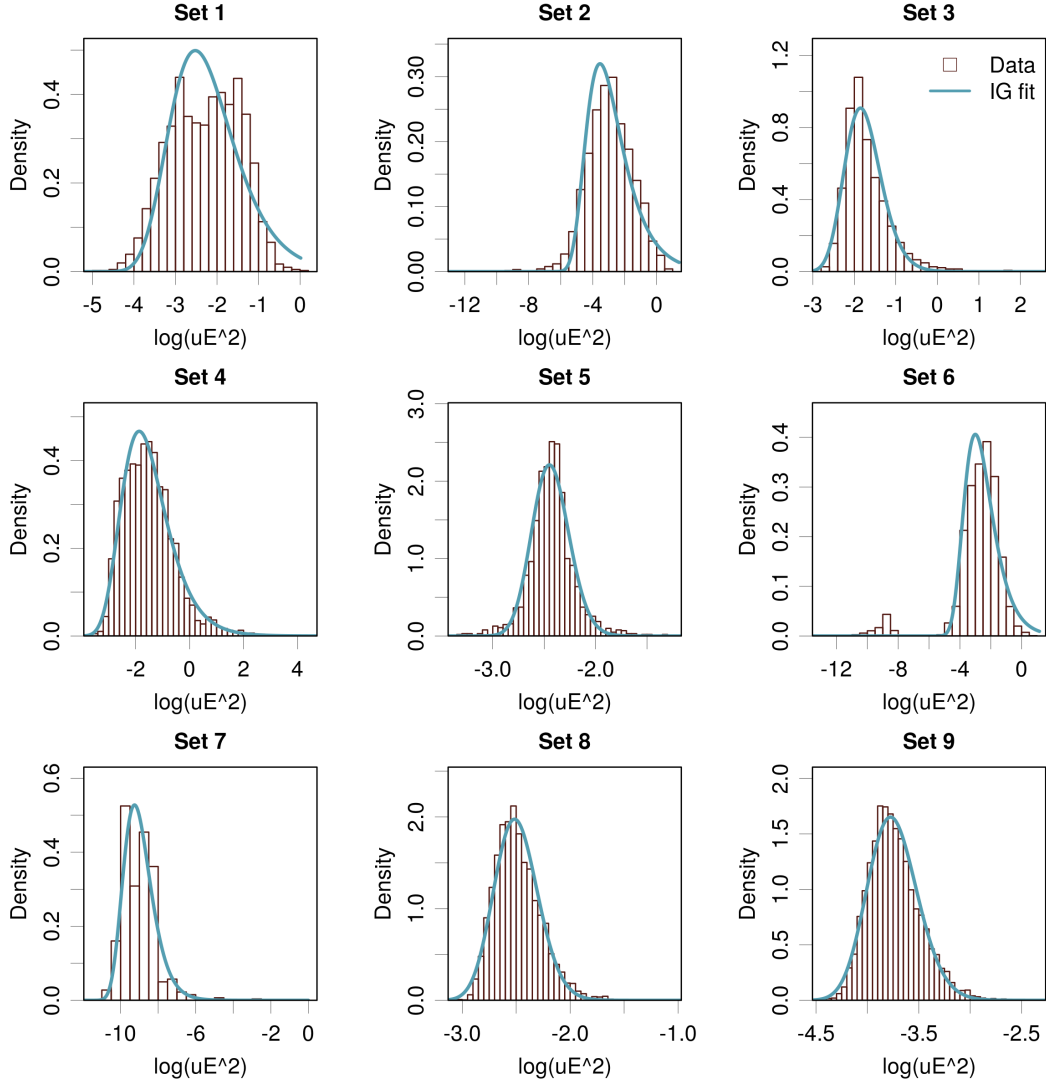


Figure 1. Fit of the squared errors (histogram) by an Inverse-Gamma  $\Gamma^{-1}(\nu, \nu)$  distribution (blue line).

This distributions is often used in Bayesian inference as a conjugate prior for the variance in a normal likelihood.

Fit of squared uncertainty distributions by the IG model is done by maximum goodness-of-fit estimation using the Kolmogorov-Smirnov distance<sup>21</sup>. The results are shown in Fig. 1, and the shape parameters reported in Table I.

Overall, the fits are rather good. The distributions for Sets 1, 2 and 6 are the worst ones, mostly due to the presence of a bimodality in these datasets (a tiny one for Set 2). The  $\nu$  values for these sets are very low: for Set 2  $\nu < 1$  corresponds to an IG distributions with undefined mean value, whereas for Sets 1 and 6 values of  $\nu < 2$  indicate an undefined variance. These values should not be over-interpreted. Nevertheless, better fitted distributions present also very small shape parameters, such as Sets 4 and 7, meaning that such values

might not be extravagant.

One can thus characterize the variance datasets by their shape parameter  $\nu$ , which covers a wide range from 0.8 to 31 (Table I).

## B. $E^2$ distributions

Using the generative model, Eq. 1, with a standard normal distribution [ $D = N(0, 1)$ ] and an IG distribution of squared uncertainties  $u_E^2/\sigma^2 \sim \Gamma^{-1}(\nu/2, \nu/2)$  leads to a scale mixture distribution of errors (Eq. 2), which has the shape of a Student's- $t$  distribution with  $\nu$  degrees of freedom<sup>22,23</sup>

$$E/\sigma \sim t(\nu) \quad (18)$$

This scale mixture is a sub-case of the Normal-IG (NIG) distribution used in evidential inference.<sup>24</sup> For the squared errors, one gets

$$E^2/\sigma^2 \sim F(1, \nu) \quad (19)$$

where  $F(\nu_1, \nu_2)$  is the Fisher-Snedecor ( $F$ ) distribution<sup>20</sup> with degrees of freedom  $\nu_1$  and  $\nu_2$ .

The squared error datasets have been fitted by a scaled  $F$  distribution, and the results are reported in Fig. 2 and Table I. The fits are very good for all sets, except for Set 6, where a minor mode at small errors is not accounted for by the  $F$  distribution. Here again, the shape parameters cover a wide range, from 0.8 to 10.

It has to be noted that, although the fits are good, the shape parameter for  $E^2$  is never close to be twice the shape parameter for  $u_E^2$  as suggested by the NIG model. The densities expected from the NIG model as plotted in Fig. 2 (red lines) for comparison with the actual fits and confirm the discrepancy. Therefore, either the generative distribution  $D$  is never close to a normal for the studied datasets, or the datasets are not properly calibrated.

## C. $Z^2$ distributions

The shape parameters for the fit of  $Z^2$  distributions by the same procedure as for  $E^2$  are reported in Table I. The fits present the same features as  $E^2$  fits (not shown), albeit with typically larger shape parameters, ranging from 0.9 to 20, which is expected from the generative model. Two exceptions are Sets 5 and 8, for which the shape parameter is slightly smaller for  $Z^2$  than for  $E^2$ , which might not be a significant difference.



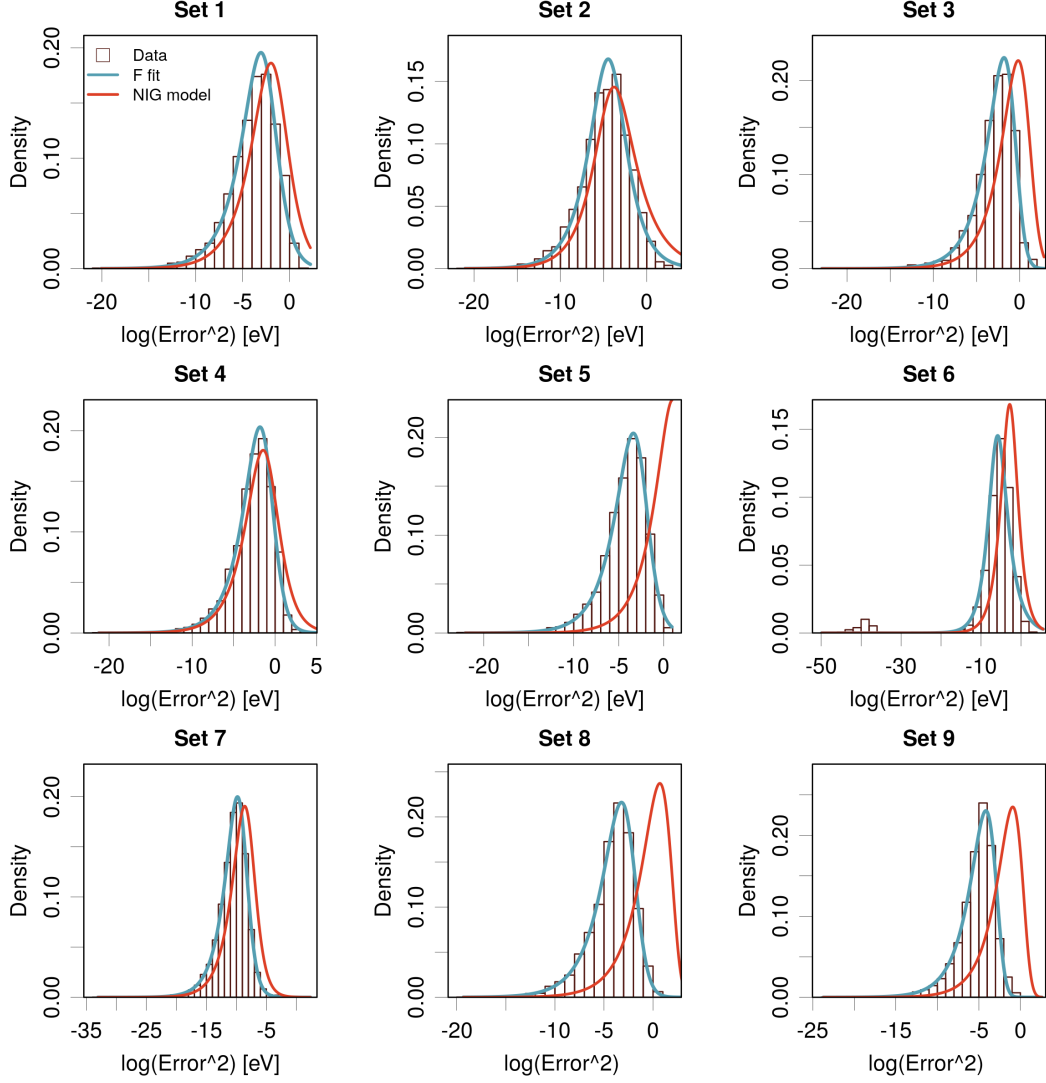


Figure 2. Fit of the squared errors (histogram) by a Fisher-Snedecor  $F(1, \nu)$  distribution (blue line). The red curves represent the distributions for NIG model compatible with Fig. 1.

#### D. Summary

This section showed that it was possible to represent the distribution of  $u_E^2$  sets by an IG distribution with reasonable accuracy, except for bimodal distributions, and that some of these distributions have very small shape parameters indicating very heavy tails. The  $E^2$  and  $Z^2$  distributions were successfully fit by F distributions, some with very small shape parameters indicating heavy tails, but the optimal shape parameters did not conform with the constraints of the NIG model.

The next section demonstrates that the presence of heavy tails in either of these quantities might challenge the reliable estimation and validation of calibration statistics.

## IV. NUMERICAL EXPERIMENTS

The characteristic features of the nine datasets presented in the previous sections are now used to design numerical experiments to assess the impact of the distributions tails on the reliability of calibration statistics. A first step is to define tailedness metric independent of model distributions.

### A. Alternative tailedness metrics

The shape of the uncertainty and error distributions can rather well be characterized by a shape parameter  $\nu$ , but one has to take into account that not all datasets are correctly fitted by the model distributions. Besides, for the  $IG$  and  $t$  distributions, shape metrics such as skewness and kurtosis are not defined for  $\nu \leq 3$  or  $4$ , respectively. One therefore needs distribution-agnostic metrics able to characterize the shape of these distributions.

Considering the asymmetric shape of  $u_E^2$ ,  $E^2$  and  $Z^2$  distributions, one might want to describe the length of the upper tail by skewness and/or the heaviness of the tails by kurtosis. For such distributions, these metrics are expected to be correlated<sup>25</sup>, but they might still provide complementary information.

As one is potentially dealing with heavy-tailed distributions and outliers, it is essential to use robust statistics.  $\beta_{GM}$  is a skewness statistic based on the scaled difference between the mean and median<sup>25-28</sup>, which is robust to outliers, varies between -1 and 1 and is null for symmetric distributions. For kurtosis,  $\kappa_{CS}$  is chosen for the same reasons<sup>25-28</sup>. This is an excess kurtosis, meaning that positive values indicate tails that are heavier than those of the normal distribution.  $\kappa_{CS}$  is not scaled and does not have finite limits.

Fig. 3 shows the correspondence between  $\nu$ ,  $\beta_{GM}$  and  $\kappa_{CS}$  for samples of the  $IG$  distribution [ $X^2 \sim \Gamma^{-1}(\nu/2, \nu/2)$ ] and  $F$ -distribution [ $X^2 \sim F(1, \nu)$ ]. There is a monotonous correspondence between  $\beta_{GM}$ ,  $\kappa_{CS}$  and the  $\nu$  parameter of the sampled distributions showing that the skewness and kurtosis statistics can be used to replace unambiguously the shape parameter of the model distributions.

Note that the coefficient of variation  $c_v$  is often used in ML-UQ studies to quantify the dispersion of uncertainties<sup>29</sup>, which is also somehow related to the tailedness of their distribution. However, it is not robust and cannot replace the proposed statistics. In the following,  $\beta_{GM}$  and  $\kappa_{CS}$  are used (and compared) to characterize the tailedness of the distributions.

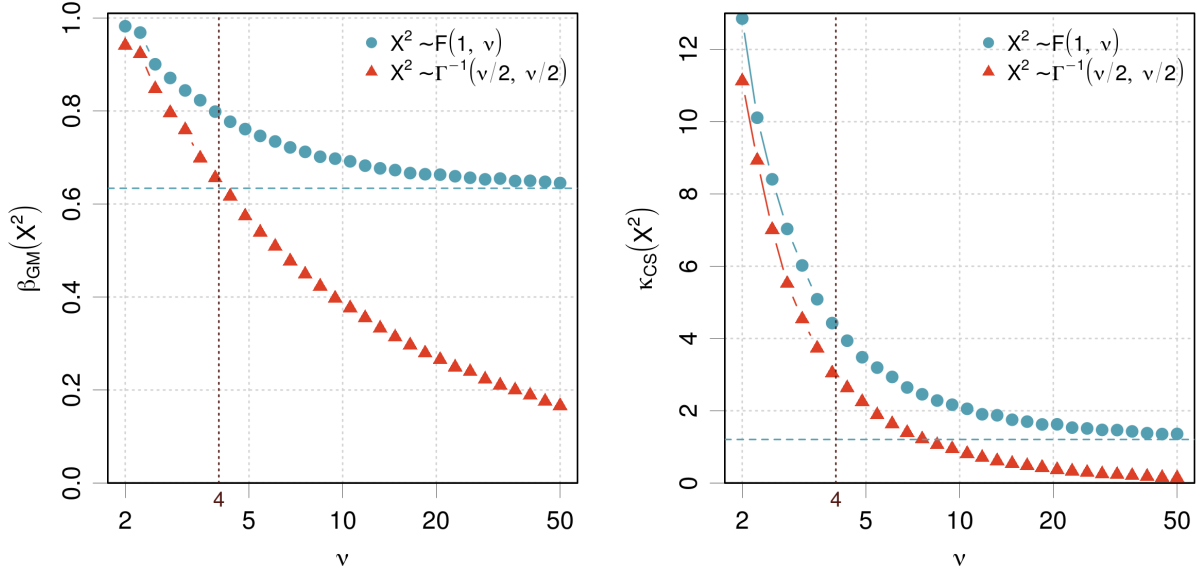


Figure 3.  $\beta_{GM}$  skewness and  $\kappa_{CS}$  kurtosis values for samples (size  $5 \times 10^5$ ) issued from Fisher-Snedecor  $F(1, \nu)$  distributions (blue dots) and from Inverse-Gamma  $\Gamma^{-1}(\nu/2, \nu/2)$  distributions (red triangles). The dashed horizontal line represents the limit for a squared normal variate.

## B. Sensitivity of calibration statistics to heavy-tailed uncertainty and error distributions

To characterize the sensitivity of the RCE and ZMS statistics to the shape of the uncertainty and error distributions in a validation context, a comparison of the rates of failure of validation tests for both statistics is performed on synthetic datasets.  $N = 10^3$  synthetic calibrated datasets of size  $M = 5000$  are generated using two scenarios designed to cover the range of distributions observed in the previous section:

- NIG - a normal generative distribution [ $D = N(0, 1)$ ] and an Inverse Gamma distribution for  $u_E^2$  [ $u_E^2 \sim \Gamma^{-1}(\nu_{IG}/2, \nu_{IG}/2)$ ], with  $\nu_{IG}$  varying between 2 and 10. Values of  $\nu_{IG}$  smaller than 2 have been avoided as they might result in numerical problems.
- TIG - a scaled Student's- $t$  generative distribution

$$D = t_s(\nu_D) := t(\nu_D) \sqrt{\frac{\nu_D - 2}{\nu_D}} \quad (20)$$

with  $\nu_D$  varying between 2.1 and 20, and a fixed Inverse Gamma distribution for  $u_E^2$  [ $u_E^2 \sim \Gamma^{-1}(3, 3)$ ]. This scenario aims to reproduce the error distributions with small shape parameters  $\nu$  that are not accessible directly by the NIG model.

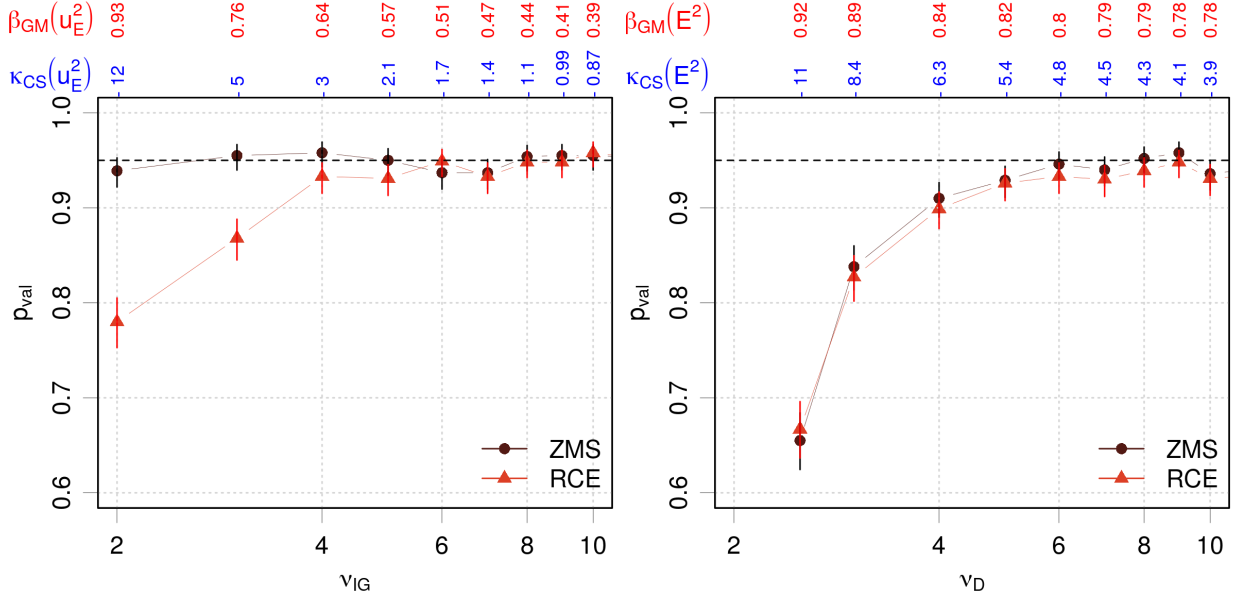


Figure 4. Validation probability of the ZMS and RCE statistics for calibrated datasets generated by two scenarios: (left) NIG with  $\nu_{IG}$  as parameter of the IG distribution; (right) TIG with  $\nu_D$  as parameter of the generative  $D = t_s$  distribution. The corresponding values of  $\beta_{GM}$  and  $\kappa_{CS}$  are reported on the upper axis.

For each sample, the calibration is tested by  $|\zeta| \leq 1$  and a probability of validity is estimated as

$$p_{val} = \frac{1}{N} \sum_{i=1}^N \mathbf{1}(|\zeta|_i \leq 1) \quad (21)$$

where  $\mathbf{1}(x)$  is the indicator function with values 0 when  $x$  is false, and 1 when  $x$  is true.

The values of  $p_{val}$  and their 95% confidence intervals obtained by a binomial model<sup>11</sup>, are plotted in Fig. 4 for the RCE and ZMS statistics as a function of  $\nu_{IG}$  or  $\nu_D$ . The upper axis provides the average  $\beta_{GM}$  and  $\kappa_{CS}$  statistics for the generated  $u_E^2$  and  $E^2$  samples.

The study of the NIG model shows that the ZMS is not sensitive to  $\nu_{IG}$ , even for extreme uncertainty distributions, and that it provides intervals that consistently validate 95% of the calibrated synthetic datasets. For the RCE, the validation error is strongly sensitive to  $\nu_{IG}$  for values below 4, reaching more than 20% for  $\nu_{IG} = 2$ . When considering the TIG model, one sees that both statistics are similarly sensitive to the shape of the generative distribution, and that the validation intervals begin to be unreliable for  $\nu_D < 6$ . The failure rate reaches over 30% for  $\nu_D = 3$ . In this case, when  $\nu_D$  diminishes, the dispersion of the generated  $\langle E^2 \rangle$  or  $\langle Z^2 \rangle$  values increases, which is not in itself a problem, but the bootstrapped CIs are unable to capture correctly this effect by being too narrow, i.e. too frequently excluding the true mean value of the distribution.

Variable	$\beta_{GM}$	$\kappa_{CS}$	Impacted stats
$u_E^2$	0.6	3.0	RCE
$E^2, Z^2$	0.8	5.0	RCE, ZMS

Table II. Limits for the skewness and kurtosis metrics above which the reliability of the RCE or ZMS metrics should be questioned.

For further reference one defines safety thresholds for the skewness and kurtosis metrics. Based on the data in Fig. 4, the limit values above which one can suspect the reliability of the calibration statistics are given in Table II. Note that these values are indicative and result from the distribution shapes observed for the studied datasets. The values for other distribution shapes might slightly differ.

### C. Summary

This section was designed to illustrate how the calibration statistics and their validation diagnostic are sensitive to the shape of the uncertainty and error distributions. The main problem is the sensitivity of the mean square (MS) statistic  $\langle X^2 \rangle$ , which is central to the studied RCE and ZMS, to the presence of outliers or heavy tails in the distribution of  $X$ . This is a well known issue, which justifies often the replacement of the root mean squared error RMSE by the more robust mean unsigned error (MUE) in performance analysis<sup>25,30</sup>. Unfortunately the use of the MS in average calibration statistics derives directly from the probabilistic model linking errors to uncertainties (Eq. 1), and one has to deal with its limitations, unless one is ready to change of uncertainty paradigm, using for instance prediction intervals or distributions.

The robust skewness ( $\beta_{GM}$ ) and kurtosis ( $\kappa_{CS}$ ) estimators were proposed and compared here as tailedness metrics, and safety limits for both metrics have been derived to help in screening out datasets with potentially unreliable RCE/ZMS values. It has been shown that heavy-tailed uncertainty distributions affect mostly the RCE, while both RCE and ZMS are affected by heavy-tailed error distributions. The ZMS benefits also from the fact that the distribution of  $Z^2$  has often lighter tails than the distribution of  $E^2$ . The next section illustrates these features on the nine example ML-UQ datasets.

Set #	$\beta_{GM}(u_E^2)$	$\kappa_{CS}(u_E^2)$	$\beta_{GM}(E^2)$	$\kappa_{CS}(E^2)$	$\beta_{GM}(Z^2)$	$\kappa_{CS}(Z^2)$
1	0.40	-0.20	<b>0.82</b>	<b>5.06</b>	0.73	2.32
2	<b>0.72</b>	<b>4.10</b>	<b>0.94</b>	<b>19.68</b>	<b>0.83</b>	<b>6.37</b>
3	<b>0.66</b>	<b>3.19</b>	0.74	2.19	0.69	1.48
4	<b>0.74</b>	<b>5.67</b>	<b>0.82</b>	4.52	0.69	2.07
5	0.19	1.84	0.78	4.32	0.79	4.07
6	0.50	1.46	<b>0.96</b>	<b>22.70</b>	<b>0.95</b>	<b>23.97</b>
7	<b>0.93</b>	<b>3.91</b>	<b>0.98</b>	<b>9.84</b>	0.78	3.97
8	0.30	0.41	0.79	4.77	0.78	4.69
9	0.30	0.48	0.77	<b>5.06</b>	0.75	4.48

Table III. Robust skewness and kurtosis values for  $u_E^2$ ,  $E^2$  and  $Z^2$ . Values above the proposed safety limits (Table II) are in bold type.

## V. APPLICATION TO THE ML-UQ DATASETS

The validation approach presented above is applied to the datasets presented in Sec. III. First, the datasets are characterized by their skewness/kurtosis values to validate the analysis of shape parameters reported above. Then, the comparison of calibration diagnostics for the RCE and ZMS is shown and analyzed. Finally, the impact on binned calibration statistics is evaluated.

### A. Skewness and kurtosis analysis

The first step is to assess the tailedness of the uncertainty, error and  $z$ -score distributions to reveal potentially problematic datasets. The corresponding  $\beta_{GM}$  and  $\kappa_{CS}$  values are reported in Table III.

The skewness and kurtosis metrics provide essentially identical diagnostics about potentially problematic datasets, the exception being Set 9 which has an error distribution slightly below the skewness limit and slightly above the kurtosis limit. For the remaining sets, one might concentrate on skewness.

The  $\beta_{GM}$  values reported in Table III indicate that some distributions present heavy tails. For uncertainties,  $\beta_{GM}(u_E^2)$  exceed 0.6 for Sets 2, 3, 4, and 7. This list conforms to the shape analysis of Table I, except for Set 6, which had a very small  $\nu$  parameter but has a moderate skewness. For the errors, the largest values occur for Sets 1, 2, 4, 6 and 7, a list where the

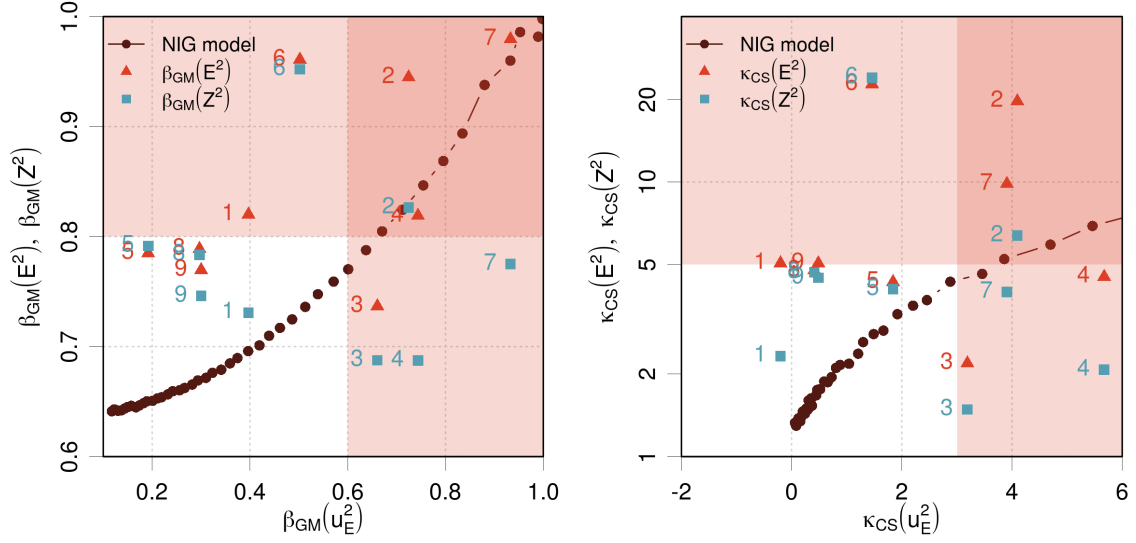


Figure 5. Skewness (left) and kurtosis (right) analysis of the application datasets. The black dots figure the NIG model for  $2 \leq \nu \leq 20$ . The colored areas signal the values that might be associated with problems.

shape analysis of Table I would have added Set 5. For the  $z$ -scores, only two sets are screened out, Sets 2 and 6, while Sets 5 and 6 have small  $\nu$  values. The correspondence between the previous shape analysis and the skewness/kurtosis screening is not perfect, which reflects the imperfect quality of the distributions fits provided by the IG and F models. According to the present analysis, Sets 1, 2, 3, 4, 6 and 7 are potentially problematic, Set 1 being very close to the limits for both skewness and kurtosis.

A graphical summary of the skewness and kurtosis analysis is provided in Fig. 5. Skewness is represented in Fig. 5(left), where  $\beta_{GM}(E^2)$  is plotted against  $\beta_{GM}(u_E^2)$  for the nine datasets (red triangles) and for the NIG model ( $2 \leq \nu \leq 20$ ; black dots). One sees directly that only Sets 5, 8 and 9 are in the safe area for both statistics, although they lie close to the  $E^2$  skewness limit. All the other sets have a skewness value that might be problematic for at least one of  $u_E^2$  or  $E^2$ . It is also noteworthy that most  $\beta_{GM}(E^2)$  values (except for Sets 3, 4 and 7) exceed what should be expected from the NIG model, confirming the shape analysis of Sect. III.

The blue squares depict the values for  $\beta_{GM}(Z^2)$ : except for Sets 2 and 6, they all lie below the safety limit (0.8), and for Set 2 the value is much closer to the limit than  $\beta_{GM}(E^2)$ . This indicates that the ZMS is much less likely to be affected by estimation problems than the RCE, except maybe for Sets 2 and 6.

The kurtosis analysis provides essentially the same results [Fig. 5(right)], except for points

$\vartheta = RCE; \vartheta_{ref} = 0$					$\vartheta = ZMS; \vartheta_{ref} = 1$				
Set	$\vartheta_{est}$	$b_{BS}$	$I_{BS}$	$\zeta_{RCE}$	Set	$\vartheta_{est}$	$b_{BS}$	$I_{BS}$	$\zeta_{ZMS}$
1	0.019	2.2e-04	[-0.021, 0.055]	<b>0.47</b>	1	0.96	-2.7e-04	[0.87, 1.11]	<b>-0.27</b>
2	-0.039	5.9e-04	[-0.106, 0.020]	<b>-0.66</b>	2	0.89	-7.3e-04	[0.80, 0.999]	-1.01
3	-0.0075	-2.1e-04	[-0.054, 0.040]	<b>-0.16</b>	3	1.12	9.4e-05	[1.05, 1.2]	1.73
4	0.055	-3.9e-04	[-0.0025, 0.12]	<b>0.96</b>	4	1.23	-6.4e-04	[1.16, 1.3]	3.50
5	0.099	1.4e-04	[0.057, 0.14]	2.33	5	0.85	1.3e-04	[0.78, 0.93]	-1.84
6	0.092	9.9e-04	[0.00079, 0.16]	1.01	6	0.98	-6.2e-04	[0.85, 1.15]	<b>-0.10</b>
7	-0.26	5.5e-03	[-0.68, -0.0012]	-1.00	7	0.97	2.6e-04	[0.94, 1.01]	<b>-0.69</b>
8	0.046	1.3e-05	[0.0082, 0.077]	1.22	8	0.93	3.4e-04	[0.87, 0.99]	-1.12
9	-0.013	2.1e-04	[-0.072, 0.027]	<b>-0.33</b>	9	0.97	2.5e-04	[0.90, 1.08]	<b>-0.26</b>

Table IV. RCE and ZMS statistics and their validation results. The bold  $\zeta_x$  values indicate calibrated sets, where  $|\zeta_x| \leq 1$ .

very close to a limit.

## B. Comparison of validation scores

The statistics and bootstrapped confidence intervals have been estimated for the RCE and ZMS for all datasets with  $10^4$  bootstrap replicates. The reference values  $\vartheta_{ref}$  are 0 for the RCE and 1 for the ZMS. The resulting values and validation scores are reported in Table IV. It is clear from these results that average calibration is not satisfied by all datasets and, more problematically, that the diagnostic depends strongly on the choice of statistic.

Comparison of the absolute  $\zeta$ -scores for ZMS and RCE across the nine datasets shows a contrasted situation [Fig. 6(left)]:

- Points close to the identity line and more globally in uncolored areas, are the datasets for which both statistics agree on the calibration diagnostic, i.e. positive for Sets 1 and 9, and negative for Set 5 and 8.
- Sets 6 and 7 are validated by the ZMS and rejected by the RCE, although very close to the limit.
- Finally, Sets 2, 3 and 4 are validated by RCE and rejected by ZMS.

Globally, the statistics disagree on more than half of the datasets, which is surprising for two statistics deriving analytically from the same generative model (Eq. 1). Considering that the



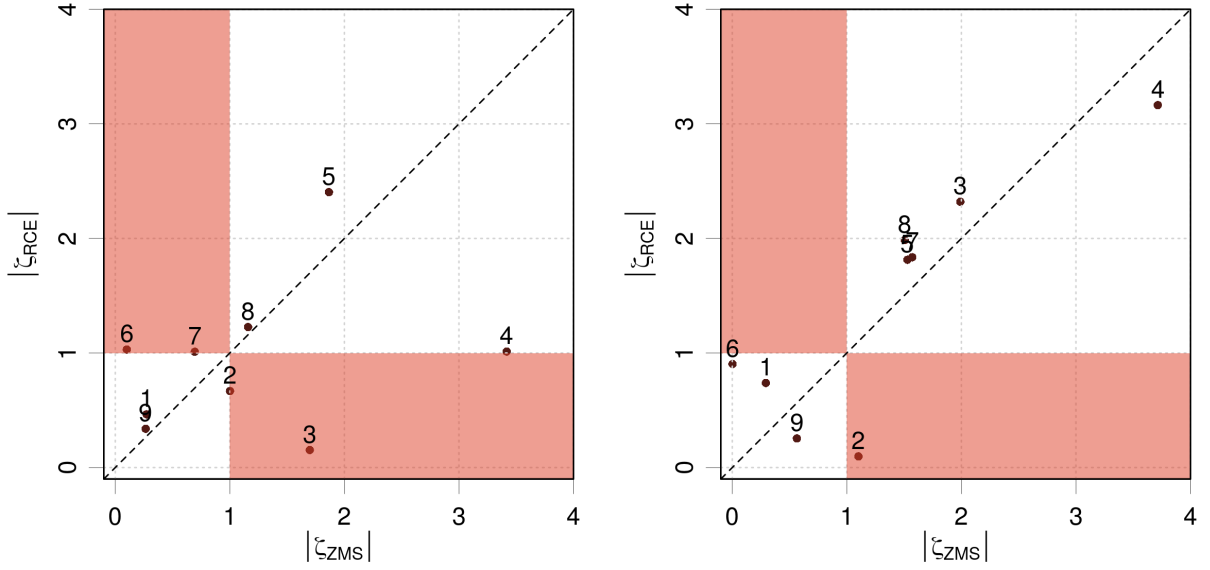


Figure 6. Comparison of the absolute  $\zeta$ -scores for ZMS and RCE: (left) the original datasets; (right) after removal of the 5% largest uncertainties. The symbols represent the set numbers in Table IV. The colored areas contain the disagreeing validation results.

RCE does not involve the pairing of uncertainties and errors implicit in the ZMS, one could have expected it to be more forbidding, which is the case for Sets 2, 3 and 4, but not for Set 6 (maybe also Sets 5 and 7).

It is remarkable that the five sets for which a disagreement between RCE and ZMS is observed (Sets 2, 3, 4, 6 and 7) are those with the largest skewness values for  $u_E^2$  (Table III, Fig. 5), with  $\beta_{GM}(u_E^2) \geq 0.6$ , except for Set 6, as shown in Fig. 5(left). This suggests that the right tail of the uncertainty distribution plays a major role in this disagreement. Sets 2, 4, 6 and 7 present also  $\beta_{GM}(E^2) \geq 0.8$ , which might point to problematic error distributions.

The role of the tails of the uncertainty and error distributions is assessed in the next section.

### C. Role of the distributions tails

In order to better understand the discrepancy of the validation results by RCE and ZMS, one needs to consider the sensitivity of these statistics to the uncertainty distributions, and notably to the large, sometimes outlying, values, as suggested by the skewness and kurtosis analyses. In the z-scores, these large uncertainty values are likely to contribute to small absolute values of  $Z$  having a small impact on the ZMS, while they are likely to affect significantly the estimation of the RCE. This hypothesis is tested on the nine datasets by a

decimation experiment, where both statistics are estimated on datasets iteratively pruned from their largest uncertainties.

The deviations of the ZMS and RCE scores from their value for the full dataset are estimated for an iterative pruning (decimation) of the datasets from their largest uncertainties, as performed in confidence curves<sup>31</sup>. The values of  $\Delta_{RCE} = RCE_k - RCE_0$  and  $\Delta_{ZMS} = ZMS_k - ZMS_0$  for a percentage  $k$  of discarded data varying between 0 and 10 % are shown in Fig. 7, where zero-centered bootstrapped 95 % CIs for both statistics are displayed as vertical bars to assess the amplitude of the deviations.

It appears that in all cases ZMS is less or as sensitive as RCE to the large extremal uncertainty values and that its decimation curve always strays within the limits of the corresponding CI. For RCE, one can find cases where it is more sensitive than ZMS but lies within the limits of the CI (Sets 2 and 6) and cases where it strays beyond the limits of the CI (Sets 3, 4 and 7). These five cases are precisely those where the RCE diagnostic differs the most from the ZMS (Sect. V B). This sensitivity test confirms the hypothesis that RCE is more sensitive than ZMS to the upper tail of the uncertainty distribution, to a point where its estimation might become unreliable.

For some sets (2, 3, 6 and 7) a small percentage (1-4 %) of the largest uncertainties affects the  $\Delta_{RCE}$  statistic, after which one observes a sharp change of slope, and the curves becomes a reflected image of the  $\Delta_{ZMS}$  statistic. These points might therefore be considered as outlying values. By contrast, one observes for Set 4 a smooth transition, which suggest that the shape of the tail is involved, more than a few extreme uncertainty values.

The sensitivity of the  $\zeta$ -scores to the removal of the 5 % largest uncertainties is shown in Fig. 6(right). One can expect from this truncation a better agreement of ZMS and RCE for those datasets with heavy  $u_E$  tails. The agreement is indeed notably improved for Set 3, 4 and 7.

Surprisingly, the  $\zeta_{RCE}$  values for Sets 2 and 6 do not follow the same trend, with a deterioration for Set 2 and no notable change for Set 6. The main reason for the discrepancy of validation metrics for Sets 2 and 6 is therefore not the shape of the uncertainty distributions, which leads us to the error distributions. Note that these are the sets for which the  $\Delta_{RCE}$  curve does *not* stray notably out of the corresponding CI limits. Both datasets present very large error skewness values  $\beta_{GM}(E^2)$  (0.92 and 0.96) and kurtosis values  $\kappa_{CS}$  (19.7 and 22.7), well above their respective safety limits. The skewness of z-scores  $\beta_{GM}(Z^2)$  for these sets (0.83 and 0.95), although smaller than  $\beta_{GM}(E^2)$ , are also above the safety limit. In comparison, the kurtosis for  $\kappa_{CS}(Z^2)$  for Set 2 (6.4) is much smaller than for Set 6 (24.0), while still

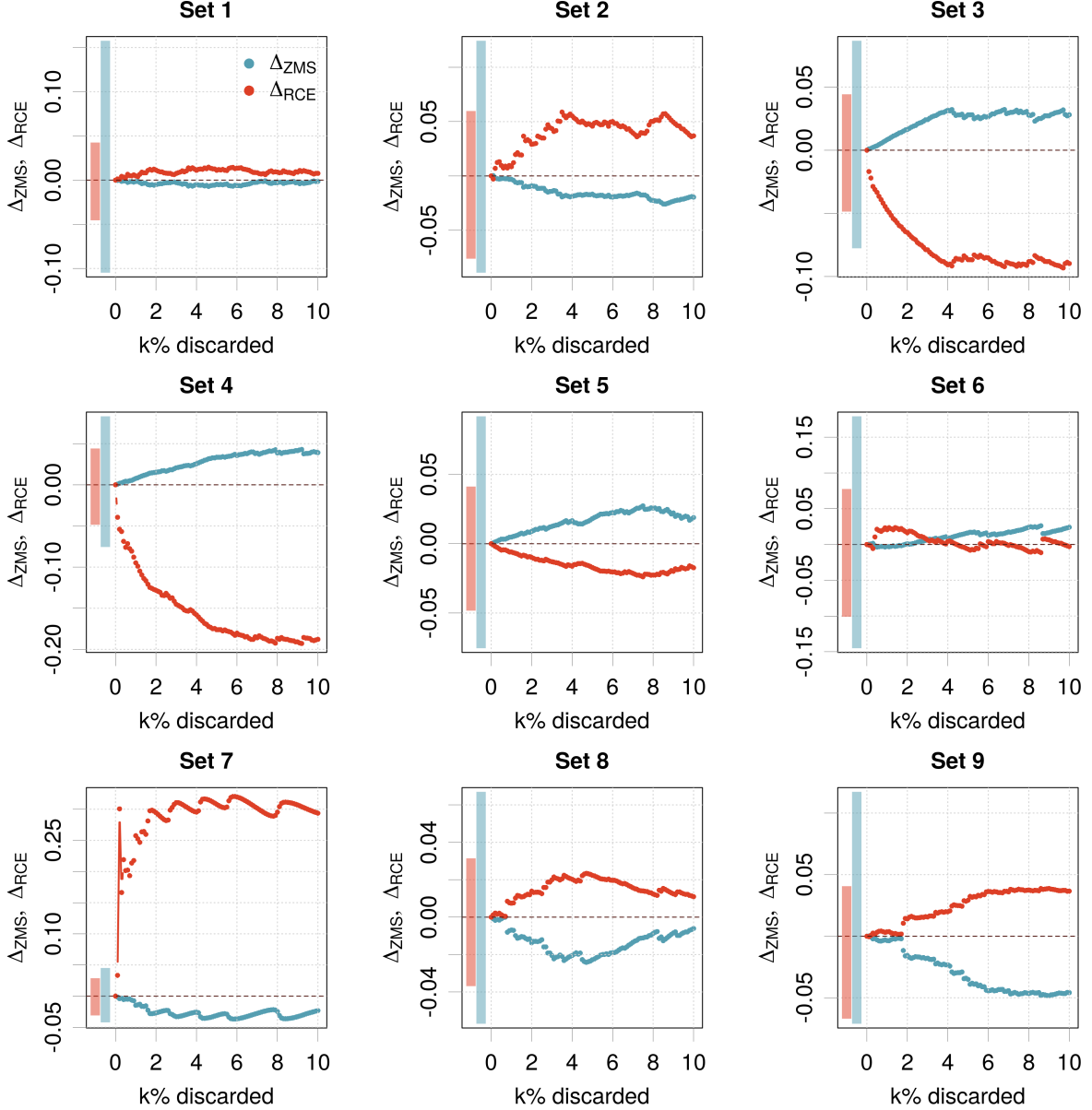


Figure 7. Variation of the RCE and ZMS statistics according to the percentage  $k$  of largest uncertainties removed from the datasets. The vertical colored bars represent 95% confidence intervals on the statistics for the full datasets.

above the safety limit (5.0). It is therefore difficult to conclude on the average calibration of Sets 2 and 6, as both the RCE and ZMS are likely to be affected by the heavy-tails of the  $E^2$  and  $Z^2$  distributions, respectively.

#### D. Impact of binning on tailedness metrics

The previous findings for average calibration statistics might also impact the reliability of *conditional* calibration. The UCE and ENCE statistics are also based on the comparison of  $MV$

to  $MSE$ , but, being bin-based, they might be less susceptible to be affected by this sensitivity issue when the binning variable is  $u_E$ . For a large enough number of bins, the problem of heavy tails or large outlying  $u_E$  values should vanish for individual bins. However, this is not necessarily the case for the corresponding error and z-scores subsets, and one might still be left with unreliable binned RCE statistics.

To assess the impact of  $u_E$ -binning on the tailedness statistics  $\beta_{GM}$  and  $\kappa_{CS}$  of the binned data, they were estimated for a set of 20 equal-sized bins and reported in Fig.8. The bins number is chosen to avoid small bins which might cause additional statistical reliability problems. The boxplots show the dispersion of the statistics of the 20 bins of  $u_E^2$ ,  $E^2$  and  $Z^2$ , while the red points locate the corresponding statistic for the full dataset.

As expected for the binned  $u_E^2$  variable, the improvement of both  $\beta_{GM}$  and  $\kappa_{CS}$  is remarkable, and all statistics get below the safety limit (red dashed line), except for a few rare outliers. Skewness lies around zero, and kurtosis gets negative values, reflecting the nearly rectangular or truncated shape of the binned  $u_E^2$  distributions. A notable exception is Set 7, which has stratified uncertainty values resulting from an isotonic regression calibration treatment<sup>32</sup>. The splitting of such a comb-like distribution into equal-size bins might result into pathological discrete distributions, as evidenced from the boxplots. This binning problem has been explored in a previous study<sup>2</sup>.

Concerning the binned errors, one can see that the effect on  $\beta_{GM}(E^2)$  is set-dependent and that there is no overall trend. Some binned datasets get an improvement and get below the safety limit (Sets 3 and 4), others get an improvement but stay at least partly above the safety limit (Sets 2, 5 and 7) and some do not get any notable improvement (Sets 5, 6, 8 and 9), or even a degradation as some bins get over the safety limit (Sets 5 and 8). The observations are globally similar for kurtosis, with again a very large dispersion for Set 7, aggravated by the occurrence of an infinite kurtosis value (not shown).

The z-scores do not benefit from a noticeable improvement for any set, and for all datasets the tailedness values get dispersed around the full set value. In consequence, even for *a priori* non-problematic datasets, a non-negligible part of the bins might rise above the safety limits. The slight improvement that can be seen on skewness for Sets 1, 3, 4 and 5 is not observed for kurtosis.

To summarize, unless the tailedness of  $u_E^2$  is the sole problem for a dataset, one cannot expect  $u_E$  binning to alleviate the reliability problem for binned calibration statistics. Moreover, if the UCE, ENCE or LZMS analysis are based on another binning variable than uncertainty (such as an input feature), as is requested to test *adaptivity*<sup>2</sup>, there is no reason

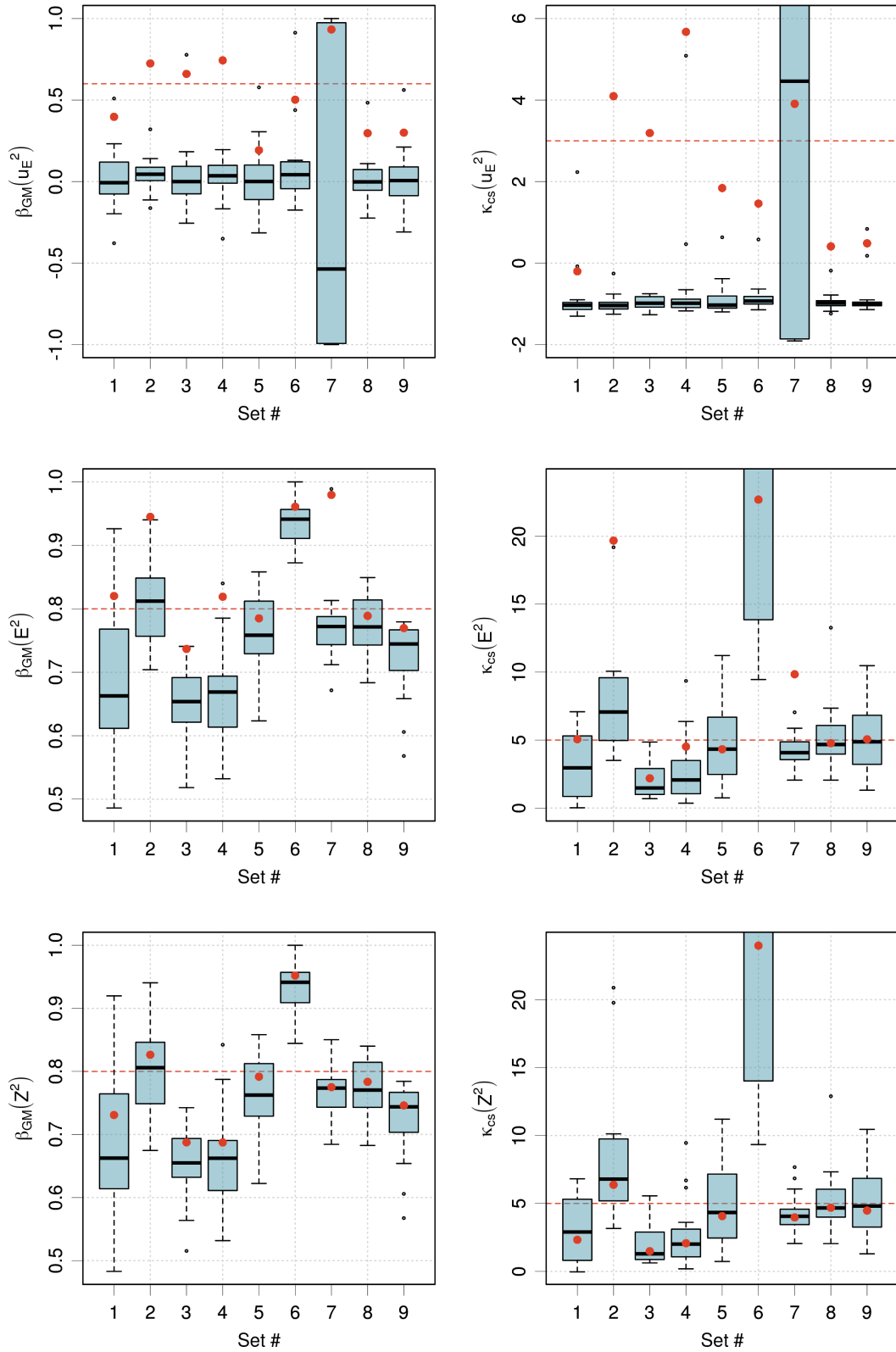


Figure 8. Impact of binning on the tailedness parameters of the binned data (20 bins). The red points locate the corresponding statistic for the full dataset. The red dashed line is the safety limit provided in Table II.

for an improvement of the binned distributions for any of  $u_E^2$ ,  $E^2$  and  $Z^2$ . In consequence, if a dataset has excessive tailedness statistics, there is no fundamental reason for conditional calibration to be more reliable than average calibration.

## VI. CONCLUSIONS

This study used the RCE and ZMS average calibration statistics to illustrate the impact of heavy-tailed uncertainty and/or error distributions on the reliability of calibration statistics. These statistics have been used because they have well defined reference values for statistical validation, which is not the case of the more popular bin-based statistics, such as the ENCE.

Discrepancies of validation diagnostic was observed between both statistics for an ensemble of datasets extracted from the recent ML-UQ literature for regression tasks. This anomaly has been elucidated by showing that the RCE is very sensitive to the upper tail of the uncertainty distribution, and notably to the presence of outliers, which has been proven by a decimation experiment (5 cases out of 9). Moreover, error sets with heavy tails can also be challenging for the RCE (5 cases). The distribution of z-scores ( $Z = E/u_E$ ) appeared to be less problematic, although some heavy-tailed  $Z$  distributions have been observed (2 cases). The underlying problem is our inability to design reliable confidence intervals with a prescribed coverage for the mean of variables with heavy-tailed distributions ( $u_E^2$ ,  $E^2$  and  $Z^2$ ). Bootstrapping is presently the best approach to CI estimation for the mean of non-normal variables, and numerical experiments have shown that it fails in conditions representative of the studied datasets. A major consequence of these observations is that average calibration statistics based on the comparison of  $MSE = \langle E^2 \rangle$  to  $MV = \langle u_E^2 \rangle$  should not be blindly relied upon for the kind of datasets found in ML-UQ regression problems. The RCE is affected by both MSE and MV sensitivity to heavy tails. In contrast, the ZMS statistic has fewer reliability issues and should therefore be the statistic of choice for average calibration testing.

In this context, it is important to be able to screen out problematic datasets. It has been shown that robust skewness ( $\beta_{GM}$ ) and/or kurtosis ( $\kappa_{CS}$ ) statistics can be used for this, and safety thresholds have been defined for both statistics and for the  $u_E^2$ ,  $E^2$  and  $Z^2$  distributions. The reliability of the RCE and ZMS statistics for datasets with values exceeding these limits has to be questioned.

A temptation would be to ignore altogether average calibration statistics and to focus on conditional calibration. As the RCE, the popular UCE and ENCE statistics implement the

comparison of  $MV$  to  $MSE$ , but, being bin-based, one might expect them to be less susceptible to the above-mentioned sensitivity issue when the binning variable is  $u_E$  (consistency testing<sup>2</sup>). Unfortunately, it has been shown in this study that even if binning solves the reliability problem for  $\langle u_E^2 \rangle$ , this is not the case for  $\langle E^2 \rangle$ , leaving these conditional calibration statistics with the same reliability problem as for the RCE. This also applies to local ZMS analysis. It is therefore essential to evaluate the tailedness of the distributions before any calibration assessment.

In *post hoc* calibration, scaling factors for the uncertainties can be derived from the ZMS ( $\sigma$  scaling<sup>33</sup>, BVS<sup>34,35</sup>) or from the UCE<sup>34</sup>. So, by extension, this problem also affects *post-hoc* calibration procedures based on statistics related to the RCE, ENCE or ZMS (for instance the NLL), and those parameterized on datasets with heavy uncertainty and/or error tails might also be unreliable.

In the absence of ML-UQ methods designed to mitigate this heavy tails problem<sup>36</sup>, there is no solution to safely ensure and validate the calibration of uncertainties for heavy-tailed uncertainty and error distributions. For such datasets, the best available approach is to rely on graphical methods<sup>11,12</sup> and to derive a qualitative diagnostic. A change of uncertainty paradigm, using prediction intervals or distributions instead of standard deviations, seems presently the most promising alternative to recover a sound statistical validation framework for calibration.

## ACKNOWLEDGMENTS

I warmly thank J. Busk for providing the QM9 dataset.

## AUTHOR DECLARATIONS

### Conflict of Interest

The author has no conflicts to disclose.

## CODE AND DATA AVAILABILITY

The code and data to reproduce the results of this article are available at [https://github.com/ppernot/2024\\_RCE/releases/tag/v2.0](https://github.com/ppernot/2024_RCE/releases/tag/v2.0) and at Zenodo (<https://doi.org/10.5281/zenodo.10998413>).

## REFERENCES

- <sup>1</sup>D. Levi, L. Gispan, N. Giladi, and E. Fetaya. [Evaluating and Calibrating Uncertainty Prediction in Regression Tasks](#). *Sensors*, 22:5540, 2022.
- <sup>2</sup>P. Pernot. [Calibration in machine learning uncertainty quantification: Beyond consistency to target adaptivity](#). *APL Mach. Learn.*, 1:046121, 2023.
- <sup>3</sup>T. Gneiting and A. E. Raftery. [Strictly Proper Scoring Rules, Prediction, and Estimation](#). *J. Am. Stat. Assoc.*, pages 359–378, 2007.
- <sup>4</sup>K. Tran, W. Neiswanger, J. Yoon, Q. Zhang, E. Xing, and Z. W. Ulissi. [Methods for comparing uncertainty quantifications for material property predictions](#). *Mach. Learn.: Sci. Technol.*, 1:025006, 2020.
- <sup>5</sup>M. H. Rasmussen, C. Duan, H. J. Kulik, and J. H. Jensen. [Uncertain of uncertainties? A comparison of uncertainty quantification metrics for chemical data sets](#). *J. Cheminf.*, 15:1–17, December 2023.
- <sup>6</sup>J. Wellendorff, K. T. Lundgaard, K. W. Jacobsen, and T. Bligaard. [mBEEF: An accurate semi-local bayesian error estimation density functional](#). *J. Chem. Phys.*, 140:144107, 2014.
- <sup>7</sup>P. Pernot and F. Cailliez. [A critical review of statistical calibration/prediction models handling data inconsistency and model inadequacy](#). *AIChE J.*, 63:4642–4665, 2017.
- <sup>8</sup>V. Kuleshov, N. Fenner, and S. Ermon. [Accurate uncertainties for deep learning using calibrated regression](#). In J. Dy and A. Krause, editors, *Proceedings of the 35th International Conference on Machine Learning*, volume 80 of *Proceedings of Machine Learning Research*, pages 2796–2804. PMLR, 10–15 Jul 2018. URL: <https://proceedings.mlr.press/v80/kuleshov18a.html>.
- <sup>9</sup>P. Pernot. [Properties of the ENCE and other MAD-based calibration metrics](#). *arXiv:2305.11905*, May 2023.
- <sup>10</sup>BIPM, IEC, IFCC, ILAC, ISO, IUPAC, IUPAP, and OIML. [Evaluation of measurement data - Guide to the expression of uncertainty in measurement \(GUM\)](#). Technical Report 100:2008, Joint Committee for Guides in Metrology, JCGM, 2008. URL: [http://www.bipm.org/utis/common/documents/jcgm/JCGM\\_100\\_2008\\_F.pdf](http://www.bipm.org/utis/common/documents/jcgm/JCGM_100_2008_F.pdf).
- <sup>11</sup>P. Pernot. [The long road to calibrated prediction uncertainty in computational chemistry](#). *J. Chem. Phys.*, 156:114109, 2022.
- <sup>12</sup>P. Pernot. [Prediction uncertainty validation for computational chemists](#). *J. Chem. Phys.*, 157:144103, 2022.



- <sup>13</sup>J. Busk, M. N. Schmidt, O. Winther, T. Vegge, and P. B. Jørgensen. [Graph neural network interatomic potential ensembles with calibrated aleatoric and epistemic uncertainty on energy and forces](#). *Phys. Chem. Chem. Phys.*, 25:25828–25837, 2023.
- <sup>14</sup>W. Zhang, Z. Ma, S. Das, T.-W. Weng, A. Megretski, L. Daniel, and L. M. Nguyen. [One step closer to unbiased aleatoric uncertainty estimation](#). *arXiv:2312.10469*, December 2023.
- <sup>15</sup>T. Gneiting, F. Balabdaoui, and A. E. Raftery. [Probabilistic forecasts, calibration and sharpness](#). *J. R. Statist. Soc. B*, 69:243–268, 2007.
- <sup>16</sup>T. J. DiCiccio and B. Efron. [Bootstrap confidence intervals](#). *Statist. Sci.*, 11:189–212, 1996. URL: <https://www.jstor.org/stable/2246110>.
- <sup>17</sup>P. Pernot. [Validation of uncertainty quantification metrics: a primer based on the consistency and adaptivity concepts](#). *arXiv:2303.07170*, 2023. [arXiv:2303.07170](#).
- <sup>18</sup>G. Palmer, S. Du, A. Politowicz, J. P. Emory, X. Yang, A. Gautam, G. Gupta, Z. Li, R. Jacobs, and D. Morgan. [Calibration after bootstrap for accurate uncertainty quantification in regression models](#). *npj Comput. Mater.*, 8:115, 2022.
- <sup>19</sup>J. Busk, P. B. Jørgensen, A. Bhowmik, M. N. Schmidt, O. Winther, and T. Vegge. [Calibrated uncertainty for molecular property prediction using ensembles of message passing neural networks](#). *Mach. Learn.: Sci. Technol.*, 3:015012, 2022.
- <sup>20</sup>M. Evans, N. Hastings, and B. Peacock. *Statistical Distributions*. Wiley-Interscience, 3rd edition, 2000.
- <sup>21</sup>M. L. Delignette-Muller and C. Dutang. [fitdistrplus: An R package for fitting distributions](#). *J Stat Softw*, 64(4):1–34, 2015.
- <sup>22</sup>D. F. Andrews and C. L. Mallows. [Scale mixtures of normal distributions](#). *Journal of the Royal Statistical Society. Series B (Methodological)*, 36:99–102, 1974. URL: <http://www.jstor.org/stable/2984774>.
- <sup>23</sup>S. T. B. Choy and J. S. K. Chan. [Scale mixtures distributions in statistical modelling](#). *Aust. N.Z. J. Stat.*, 50:135–146, 2008.
- <sup>24</sup>A. Amini, W. Schwarting, A. Soleimany, and D. Rus. [Deep Evidential Regression](#). *arXiv:1910.02600*, October 2019.
- <sup>25</sup>P. Pernot and A. Savin. [Using the Gini coefficient to characterize the shape of computational chemistry error distributions](#). *Theor. Chem. Acc.*, 140:24, 2021.
- <sup>26</sup>E. L. Crow and M. M. Siddiqui. [Robust estimation of location](#). *J. Am. Stat. Assoc.*, 62:353–389, 1967.
- <sup>27</sup>R. A. Groeneveld and G. Meeden. [Measuring skewness and kurtosis](#). *The Statistician*, 33:391–399, 1984. URL: <http://www.jstor.org/stable/2987742>.

- <sup>28</sup>M. Bonato. [Robust estimation of skewness and kurtosis in distributions with infinite higher moments.](#) *Financ Res Lett*, 8:77–87, 2011.
- <sup>29</sup>G. Scalia, C. A. Grambow, B. Pernici, Y.-P. Li, and W. H. Green. [Evaluating scalable uncertainty estimation methods for deep learning-based molecular property prediction.](#) *J. Chem. Inf. Model.*, 60:2697–2717, 2020.
- <sup>30</sup>P. Pernot and A. Savin. [Probabilistic performance estimators for computational chemistry methods: the empirical cumulative distribution function of absolute errors.](#) *J. Chem. Phys.*, 148:241707, 2018.
- <sup>31</sup>P. Pernot. [Confidence curves for UQ validation: probabilistic reference vs. oracle.](#) *arXiv:2206.15272*, June 2022.
- <sup>32</sup>P. Pernot. [Stratification of uncertainties recalibrated by isotonic regression and its impact on calibration error statistics.](#) *arXiv:2306.05180*, June 2023.
- <sup>33</sup>M.-H. Laves, S. Ihler, J. F. Fast, L. A. Kahrs, and T. Ortmaier. [Well-calibrated regression uncertainty in medical imaging with deep learning.](#) In T. Arbel, I. Ben Ayed, M. de Bruijne, M. Descoteaux, H. Lombaert, and C. Pal, editors, *Proceedings of the Third Conference on Medical Imaging with Deep Learning*, volume 121 of *Proceedings of Machine Learning Research*, pages 393–412. PMLR, 06–08 Jul 2020. URL: <https://proceedings.mlr.press/v121/laves20a.html>.
- <sup>34</sup>L. Frenkel and J. Goldberger. [Calibration of a regression network based on the predictive variance with applications to medical images.](#) In *2023 IEEE 20th International Symposium on Biomedical Imaging (ISBI)*, pages 1–5. IEEE, 2023.
- <sup>35</sup>P. Pernot. [Can bin-wise scaling improve consistency and adaptivity of prediction uncertainty for machine learning regression ?](#) *arXiv:2310.11978*, October 2023.
- <sup>36</sup>Note that uncertainty sets with large dispersion (large  $c_v$  statistic) and therefore potentially heavy tails, are favored for active learning.